Corrosion Resistance of Nickel Coatings Obtained by Electrodeposition in a Sulfamate Bath in the Presence of Samarium (III)

J. R. López[1], G. Stremsdoerfer[2], G. Trejo[1], R. Ortega[1], J. J. Pérez[1], Y. Meas[1,*]

[1] Centro de Investigación y Desarrollo Tecnológico en Electroquímica (CIDETEQ), Parque Tecnológico Querétaro, Sanfandila, Pedro Escobedo, Querétaro, C.P. 76700 A.P. 064, México
[2] Ecole Centrale of Lyon, Tribological & Dynamical Systems Laboratory, 36 Avenue Guy de Collongue, P.O. Box 163, 69134 Ecully, France
[*]E-mail: yunnymeas@cideteq.mx

This work studied the effect of the addition of samarium (III) on the corrosion resistance of nickel coatings obtained from a sulfamate bath. The coatings obtained were characterized by X-ray diffraction and scanning electron microscopy (SEM). The corrosion resistance of the coatings was evaluated in 5% NaCl, employing electrochemical polarization measurement, electrochemical impedance spectroscopy and salt spray testing. The results indicated that the coatings obtained using an electrochemical bath with 24.6 mM of Sm^{3+} had a grain size of 24.4 nm. The SEM image of the cross-section of these coatings showed a microstructure with a columnar growth that was more compact than the microstructure obtained from Ni coatings untreated with samarium. Polarization curves and electrochemical impedance spectroscopy demonstrated that corrosion current density decreased and charge transfer resistance increased when the concentration of samarium in the electrolyte bath was increased. Both results agreed with those obtained from salt spray testing, which indicated that Ni coatings obtained from a bath with 24.6 mM of Sm^{3+} showed the highest corrosion resistance (6096 h).

1. INTRODUCTION

Nickel coatings obtained through electrodeposition are commonly used at the industrial level. They offer an alternative protection against corrosion and increased wear resistance in a relatively economic process. The properties of these coatings, such as corrosion resistance, are determined by their morphology, microstructure, metallic impurity content, grain size and porosity [1] characteristics

which widely depend on the composition of the electrolyte bath, current density, pH, temperature and additives.

An alternative for improving the aforementioned properties of nickel coatings is the elaboration of composite coatings. These types of coatings can be obtained using an electrolyte bath that contains metallic and non-metallic nanoparticles or microparticles suspended in the electrolyte. The incorporation of rare earth compounds into the coatings, especially of cerium oxide (CeO_2) into a nickel coating, has been shown to improve wear and corrosion resistance [2-4].

Nevertheless, the possibility of obtaining a homogenous co-deposit of these particles in a principal matrix of Ni is very complex and depends on many factors, such as particle size and uniformity of distribution in the electrolyte. Recently, a new procedure for the creation of a Ni-CeO_2 composite coating was studied through the simultaneous electrodeposition of the metal and cerium oxide without the addition of CeO_2 particles in the electrolyte bath [5].

In the present work, the aim was to study the corrosion resistance of electrodeposited nickel prepared from a sulfamate bath with different concentrations of samarium (III). The corrosion resistance of each coating was evaluated through polarization curves, electrochemical impedance spectroscopy and salt spray testing.

2. EXPERIMENTAL PROCEDURE

2.1 Materials

Electrodeposited Ni coatings of approximately 12 μm thickness were obtained from a sulfamate electrolyte bath without chloride ions and of the following composition: 400 g/L $Ni(NH_2SO_3)_2 \cdot 4H_2O$, 40 g/L H_3BO_3, 3 mL/L of a commercial surfactant (Antipitting Surfactant "AA") and different concentrations of samarium sulfate (2.7, 8.2 and 24.6 mM of Sm^{3+}). The operating conditions were: pH=2.5 (adjusted with sulfamic acid and nickel carbonate), temperature of 55 °C, a current density of 30 mA/cm^2, and using a nickel anode (high purity) and a steel sheet cathode, AISI 1006 (0.074% C, 0.004 % S, 0.008 % P, 0.245 % Si, 0.174 % Mn) of dimensions 65x70x1 mm. Prior to nickel electrodeposition, the steel plates were immersed first in an alkaline solution at 80 °C for 10 minutes and then in a solution of sulfamic acid (30 g/L) for 10 s.

2.2. Corrosion evaluation

2.2.1. Polarization curves and electrochemical impedance spectroscopy in 5% NaCl

Polarization curves were obtained using a potentiostatic technique, employing a PAR 263A potentiostat and a three-electrode cell, model PAR K0235 with a platinum mesh as the auxiliary electrode and a saturated calomel electrode (SCE) as the reference electrode. The measurements were carried out in 5% NaCl at 25 °C with a scan rate of 0.17 mV/s (according to ASTM G5). Measurement of the electrochemical impedance was performed at an open circuit potential of 10 mV from 100 KHz

to 10 mHz using a PARSTAT 2273 potentiostat. Each experiment was initiated two hours after the samples were submerged in the solution in order to guarantee equilibrium.

2.2.2. Salt spray testing

Salt spray test were performed using methods ASTM B117 and ISO 10289 in a Q-FOG CCT-600 corrosion chamber. The criterion for determining coating failure was the first sign of red corrosion.

2.3. Coating characterization

The cross section and morphologie of the surface were characterized using a scanning electron microscope (JEOL-5400LV). The texture and grain size of the electrodeposited nickel coatings were measured using X-ray diffraction with a Bruker AXS D8-Advanced diffractometer.

3. RESULTS AND DISCUSSION

3.1 Corrosion resistance evaluation

In Figure 1, the polarization curves of the coatings obtained at different Sm^{3+} concentrations are shown. Generally, Ni coatings obtained from an electrochemical bath with samarium showed more positive corrosion potentials than Ni coatings produced in the absence of samarium.
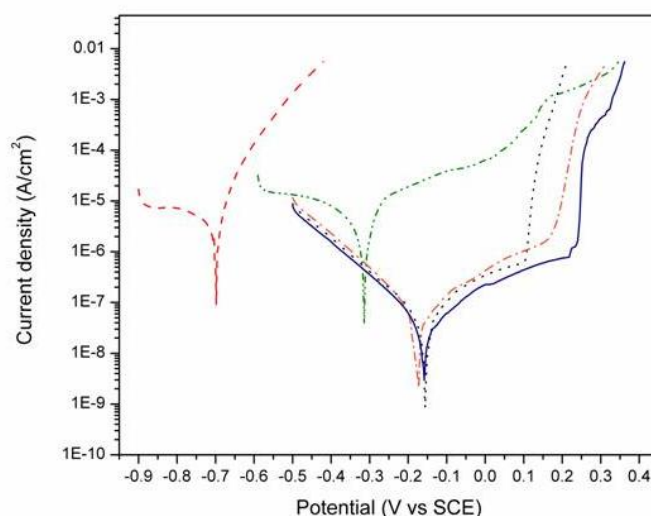

Figure 1. Polarization curves obtained in 5% NaCl for the substrate (— —) and for electrodeposited Ni prepared from an electrolyte bath using different samarium concentrations: 0 mM Sm^{3+} (— •• —), 2.7 mM Sm^{3+} (••••), 8.2 mM Sm^{3+} (— • —) and 24.6 mM Sm^{3+} (——).

The corrosion potentials did not show considerable variation (20 mV maximum difference) with increasing of samarium concentration (ranging from 2.7 to 24.6 mM). Considerable changes were observed in the oxidation reaction, however.

Excepting the substrate polarization curve, it can be observed that at potentials more positive than the corrosion potential (oxidation reaction zone), all curves show two characteristic regions: one in which the current is small, slightly increasing with the potential and indicating the presence of a passive layer, and a second region where the current increases abruptly with the potential [6]. The abrupt change in the second region is attributed to the breaking of the passive layer, followed by pitting corrosion [7,8]. The potential where this second region begins is generally known as the pitting potential (E_p) [9,10].

In Table 1, the electrochemical parameters obtained from the polarization curves are shown. The corrosion current density (j_{corr}) was calculated from the intercept at the corrosion potential (E_{corr}) from the Tafel slope for the anodic reaction, while the pitting potential was estimated from the polarization curve. A considerable decrease in corrosion current density coincides with the increase of Sm^{3+} concentration in the electrolyte bath. At Sm^{3+} concentrations higher than 8.2 mM, the corrosion current density decreases to less than 0.1 $\mu A/cm^2$ This value is one order of magnitude less than the estimated density of a Ni coating obtained without samarium (8.15 $\mu A/cm^2$)

These results also show that the critical pitting potential increases with the increase of Sm^{3+} concentration. Potentials of 0.052V and 0.25V can be observed for the coatings obtained in the absence and presence of 24.6 mM of Sm^{3+}, respectively. These results indicate that the addition of samarium allows coatings to be obtained with improved chloride pitting corrosion resistance. The incorporation of samarium compounds in the nickel coatings could favor the creation of a passive film that has higher resistance to pitting attack.

Table 1. Electrochemical parameters of the polarization curves

Sample	E_{corr} (V vs SCE)	j_{corr} ($\mu A/cm^2$)	E_p (V vs SCE)
Substrate (steel AISI 1006)	-0.698	11.69	
Ni (0 mM Sm^{3+})	-0.314	8.15	0.052
Ni (2.7 mM Sm^{3+})	-0.156	0.12	0.142
Ni (8.2 mM Sm^{3+})	-0.172	0.06	0.210
Ni (24.6 mM Sm^{3+})	-0.158	0.07	0.250

Figure 2 shows the Nyquist diagrams obtained for the Ni coatings, diagrams which show only one semicircle in the range of the frequencies studied. The presence of this semicircle is attributed to the charge transfer process in the metal-solution interface; similar results were previously reported for electrodeposited Ni in NaCl solutions [11, 12]. The behavior of these experimental values can be described by the equivalent circuit seen in Figure 3, where R_s represents the solution resistance, R_{tc} the transfer resistance and CPE the constant phase element at the interface between the metal and the

electrolyte. This type of equivalent circuit is typically utilized for these kinds of studies; the use of a CPE in place of a capacitor is attributed to the deviations caused by imperfections that are present on the coating surface [12].
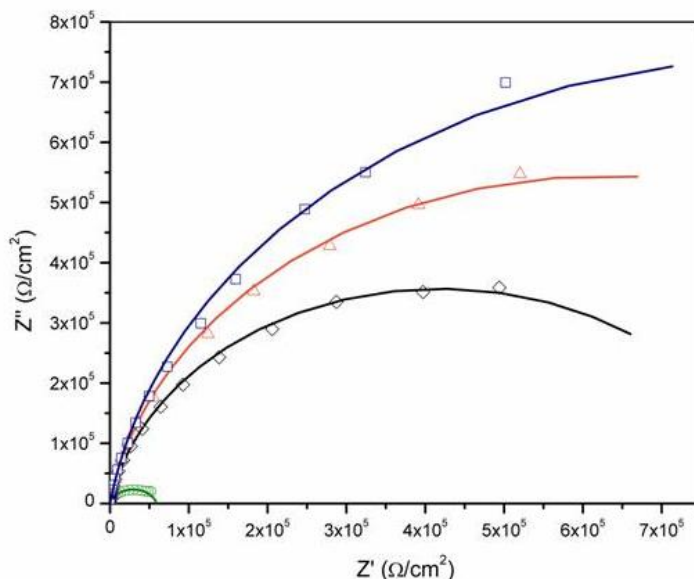

Figure 2. Nyquist diagrams obtained in 5% NaCl for electrodeposited Ni prepared from an electrolyte bath using the following samarium concentrations: 0 mM Sm^{3+} (**O**), 2.7 mM Sm^{3+} ($\lozenge$), 8.2 mM Sm^{3+} ($\triangle$) y 24.6 mM Sm^{3+} ($\square$). Simulated data from an equivalent circuit (—).

The equivalent circuit parameters were obtained using Zview software and are presented in Table 2. These parameters permit a good approximation between the values obtained by the simulation of the equivalent circuit and those obtained through experimental measures. The results obtained through this adjustment show an increase in charge transfer resistance (improved resistance to corrosion) according to samarium concentration. The value of R_{tc} is two orders of magnitude greater for the coating obtained with 24.6 mM of Sm^{3+} (1.71×10^6 Ω/cm^2) than for that obtained in the absence of samarium (5.90×10^4 Ω/cm^2).

Table 2. Parameters of the equivalent circuit obtained through modeling the impedance spectra of electrodeposited Ni in 5% NaCl

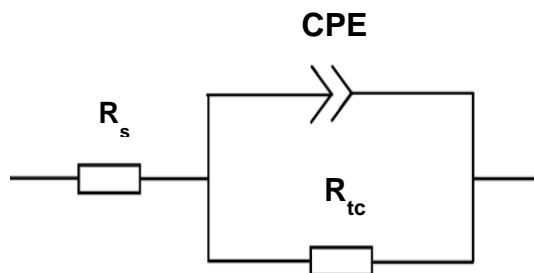| Sample	R_s (Ω cm^2)	R_{tc} (Ω cm^2)	CPE (F/cm^2)
Substrate (steel AISI 1006)	6.48	3131	5.49×10^{-4}
Ni (0 mM Sm^{3+})	6.41	5.90×10^4	3.794×10^{-5}
Ni (2.7 mM Sm^{3+})	6.98	8.38×10^5	2.50×10^{-5}
Ni (8.2 mM Sm^{3+})	6.631	1.26×10^6	2.39×10^{-5}
Ni (24.6 mM Sm^{3+})	7.318	1.71×10^6	2.29×10^{-5}

CPE

R$_s$

R$_{tc}$

Figure 3. Equivalent circuit used to simulate the electrodeposited Ni impedance spectrum in 5% NaCl.

These results are in good agreement with those from the polarization curves, indicating that corrosion resistance improves as the concentration of samarium increases. This enhanced corrosion resistance is due to the formation of a compact protective oxide film on the metal surface.

In Figure 4, the results of salt spray testing are shown for Ni coatings in the absence and presence of samarium. The beginning of corrosion in the substrate, also known as the failure time, is defined as the first point in time where red rust appears. Looking at the data, it is clear that corrosion resistance increased considerably as samarium concentration increased. These results show that the salt spray test exposure time for the Ni coating using 8.2 mM of Sm^{3+} was 2424 h, while the salt spray test exposure time for the 24.6 mM of Sm^{3+} was slightly greater than 6000 h. These results concur with the data from the polarization curves and the electrochemical impedance.
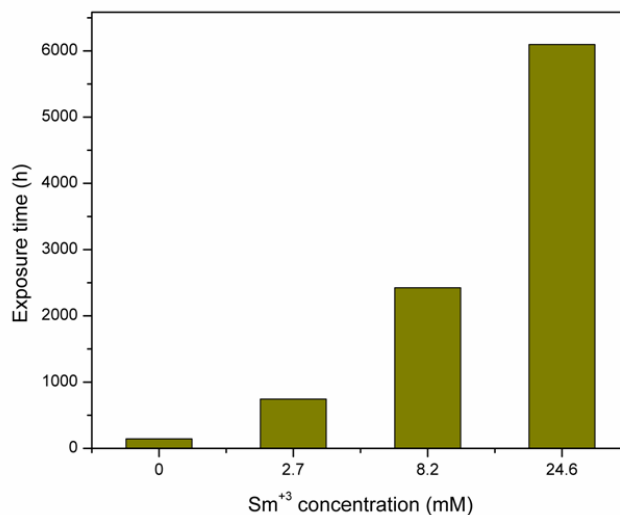
Figure 4. Salt spray test exposure results, indicating the failure times of each coating (first sign of red corrosion) as a function of samarium (III) concentration.

3.2 Characterization of the coating

X-ray diffraction spectra for the Ni coatings with and without samarium are shown in Figure 5. Both forms of electrodeposited Ni show a face-centered cubic crystalline structure with preferential

growth in the (200) plane, followed by the (111) plane, characteristics which have previously been reported for nickel coatings prepared from a sulfamate solution [12,13]. At 24.6 mM of Sm^{3+}, the peak intensity of the (200) plane decreased, and the peak intensity of the (111) plane slightly increased. The preferential orientation values, determined by the ratio $I_{(200)}/I_{(111)}$ and the grain size (calculated using Scherrer's equation), are listed in Table 3. These values show a decrease in the preferential orientation (200) and a slight decrease in the grain size for electrodeposited Ni with 24.6 mM of Sm^{3+}. This decrease in the preferential orientation can be attributed to a more compact structure, which could be due to the absorption of Sm^{3+} during Ni electrodeposition.

It is important to indicate that the X-ray diffraction studies did not show the presence of Sm^{3+} in the coatings, either due to the small quantity or because it was amorphous. Nevertheless, the X-ray diffraction spectra of the coating after exposure to salt spray testing (see Figure 6) contain a peak attributed to samarium oxides, showing the incorporation of these compounds into the electrodeposited Ni. The incorporation mechanism of these compounds could be similar to previously reported mechanisms for cerium and samarium films [14,15]. Such mechanisms are based on the generation of hydroxide ions (OH^-) in the metal-dissolution interface, which results in the reduction of a soluble precursor over the substrate surface. According to this mechanism, the Sm^{3+} first forms hydroxides and can later be transformed into oxides [14,15].
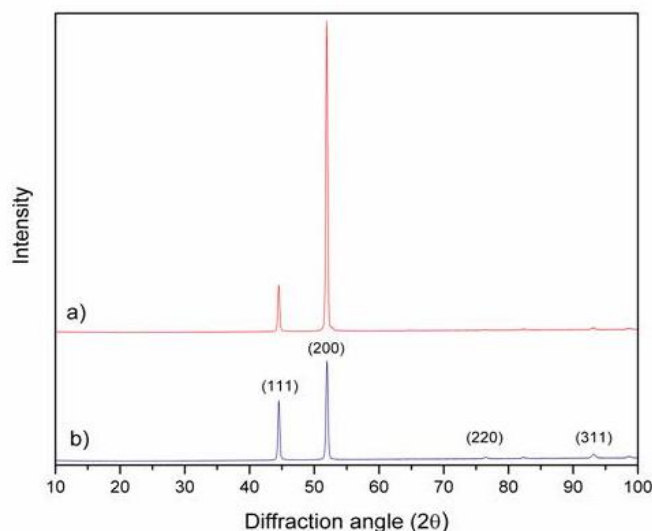

Figure 5. X-ray diffraction spectrum of electrodeposited Ni; a) 0 mM Sm^{3+} and b) 24.6 mM Sm^{3+}.

Table 3. Preferential orientation and grain size for electrodeposited Ni in the presence and absence of samarium

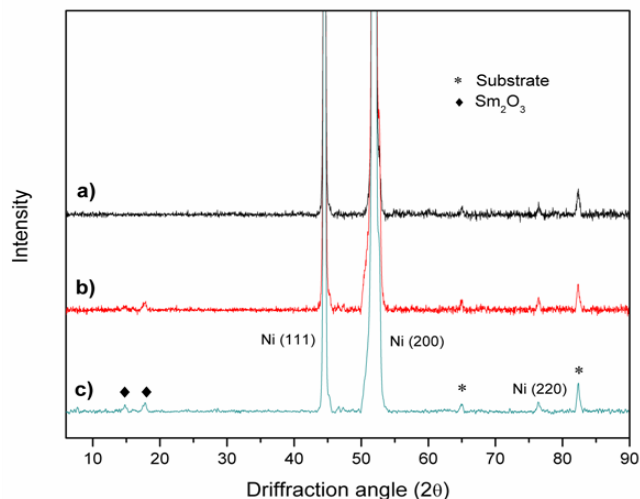| Sm^{3+} concentration	$I_{(200)}/I_{(111)}$	Grain Size (nm)
0 mM	6.55	27.3
24.6 mM	1.63	24.4

Figure 6. X-ray diffraction spectrum for electrodeposited Ni from the 24.6 mM Sm^{3+} solution after salt spray test exposure: a) 0 h, b) 96 h and c) 240 h.

Figures 7a and 7b show the surface morphologies of electrodeposited Ni in the absence and presence of samarium. Both coatings have small particles in pyramid form, while the coating of Ni in the presence of samarium shows a slightly more homogenous surface with fewer imperfections than the coating obtained without. The SEM cross-section images for these coatings are shown in Figures 7c and 7d; these images show a columnar growth that is characteristic of electrodeposited nickel from a sulfamate bath [16-18].
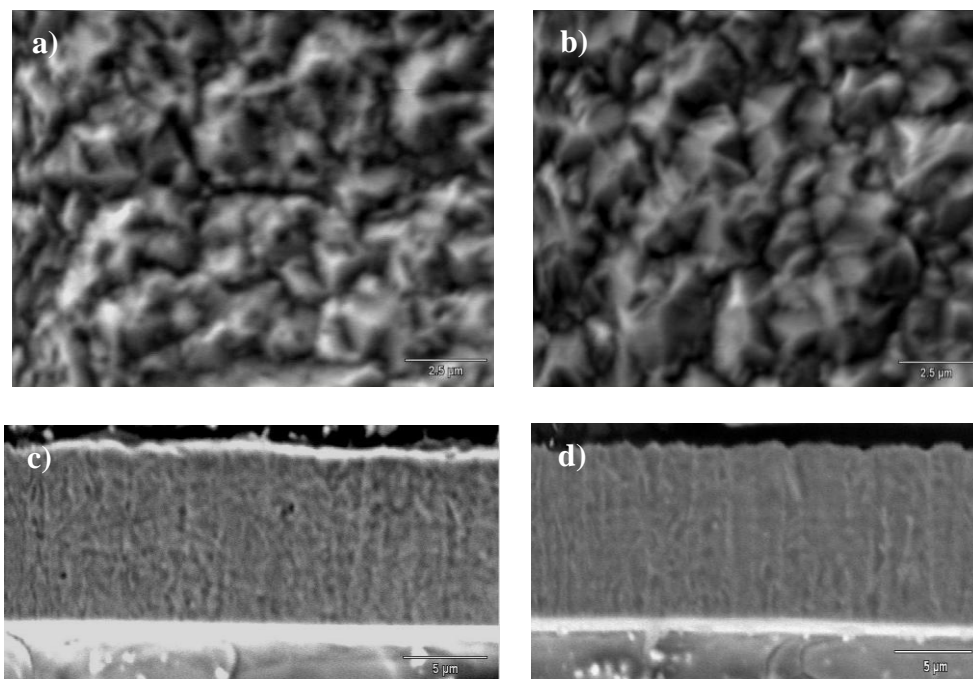

Figure 7. SEM image of the surface (10000X) and of the cross-section (5000X) of electrodeposited Ni with and without samarium; a) Ni surface w/o samarium, b) Ni surface with 24.6 mM Sm^{3+}. c) Ni cross-section w/o samarium and d) Ni cross-section with 24.6 mM Sm^{3+}.

This microstructure was observed after chemical etching with an acid solution composed of nitric acid and acetic acid (50:50 % v/v), based on information previously reported [19]. These images show a much more compact coating for the deposition that resulted from 24.6 mM Sm^{3+}, which indicates that the samarium in the electrolyte bath was incorporated into the nickel, creating more compact deposits of lower porosity and thus a considerable increase in corrosion resistance.

From the X-ray diffraction and SEM results, it can be verified that the incorporation of samarium in the electrolyte bath promotes a coating with a grain size of approximately 24 nm and a compact microstructure of columnar growth. This compact microstructure also displays fewer defects than the coatings made in the absence of samarium. This could be due to the adsorption and incorporation of samarium compounds during the Ni electrodeposition process, however more research should be carried out for a better understanding of the mechanism involved.

4. CONCLUSIONS

The testing of corrosion resistance with polarization curves, electrochemical impedance spectroscopy and salt spray testing allowed confirmation that the electrodeposited Ni obtained with 24.6 mM of Sm^{3+} presented a better corrosion resistance. The improvement in corrosion resistance is caused by the compact microstructure and the presence of rare earth compounds in the coatings incorporated during the electrodeposition process. These compounds could favor the formation of a passive film that is more resistant to chloride attack and therefore increases the corrosion resistance. It is necessary to perform further experiments that can help clarify the mechanism of protection against corrosion.

References

1. Jack W. Dini, *ELECTRODEPOSITION The Materials Science of Coatings and Substrates*, Noyes Publications, New Jersey (1993)
2. S.T. Aruna, C.N. Bindu, V. Ezhil Selvi, V.K. William Grips and K.S. Rajam, *Surf. Coat. Technol.* 200 (2006) 6871
3. Yu-Jun Xue, Xian-Zhao Jia, Yan-Wei Zhou, Wei Ma and Ji-Shun Li, *Surf. Coat. Technol.* 200 (2006) 5677
4. Baolei Han and Xinchun Lu, *Surf. Coat. Technol.* 202 (2008) 3251
5. H. Hasannejad, T. Shahrabi, M. Jafarian and A. Sabour Rouhaghdam, *J. Alloys Compd.* 509 (2011) 1924
6. F.C. Walsh, C. Ponce de León, C. Kerr, S. Court and B.D. Barker, *Surf. Coat. Technol.* 202 (2008) 5092

7. Jiaan Liu, Xianyong Zhu, Jothi Sudagar, Fei Gao and Pibo Feng, *Int. J. Electrochem. Sci*., 7 (2012) 5951
8. Jothi Sudagar, Guangli Bi, Zhonghao Jiang, Guangyu Li, Qing Jiang and Jianshe Lian, *Int. J. Electrochem. Sci*., 6 (2011) 2767
9. S.M. Abd El-Haleem, S. Abd El-Wanees, *Mater. Chem. Phys*. 128 (2011) 418–426
10. El-Sayed M. Sherif, A. A. Almajid, A. K. Bairamov and Eissa Al-Zahrani, *Int. J. Electrochem. Sci*., 7 (2012) 2796
11. QIN Li-yuan, LIAN Jian-she and JIANG Qing, *Trans. Nonferrous Met. Soc. China* 20 (2010) 82
12. Haijun Zhao, Lei Liu, Jianhua Zhu, Yiping Tang and Wenbin Hu, *Mater. Lett*. 61 (2007) 1605
13. E. Pompei, L. Magagnin, N. Lecis and P.L. Cavallotti, *Electrochim. Acta* 54 (2009) 2571
14. Edgar J. Ruiz, Raúl Ortega-Borges, Luis A. Godínez, Thomas W. Chapman and Yunny Meas-Vong, *Electrochim. Acta* 52 (2006) 914
15. V. Lair, L. S. ˇZivkoviˊc, O. Lupan and A. Ringuedé, *Electrochim. Acta* 56 (2011) 4638
16. A. Godon, J. Creus, E. Conforto, X. Feaugas and C. Savall, *Mater. Charact*. 62 (2011) 164
17. S. W. Banovic, K. Barmak and A. R. Marder, *J. Mater. Sci*. 33 (1998) 639
18. Chao-Sung Lin, Kun-Cheng Peng, Pei-Cheng Hsu, Liuwen Chang and Chih-Hsiung Chen, *Mater. Trans*., 41 (2000) 777
19. J. K. Dennis and T. E. Such, *Nickel and Chromium plating*, Third Edition, Woodhead Publishing, Cambridge (1993)